On the integration of optimal energy management and thermal management of hybrid electric vehicles

Julien Lescot and Antonio Sciarretta
IFP, 1 et 4, avenue de Bois-Préau,
92852 Rueil-Malmaison Cedex -France
Email : julien.lescot@ifp.fr

Yann Chamaillard and Alain Charlet
Institut le Prisme, rue Léonard de Vinci
45100 Orléans

***Abstract*—This paper proposes a supervisory control for hybrid electrical vehicle (HEV). It is based on Equivalent Consumption Minimization Strategy (ECMS) extended with a new state reflecting the thermal state of the engine. A new consumption law taking into account the losses due to low engine temperature is therefore included in the optimal control problem. The strategy is tested offline on a regulatory driving cycle, the results show an improvement on the consumption which confirm the relevance of the approach.**

keywords : hybrid vehicles, optimal control, Pontryagin's Principle, thermal management

I. Introduction

Energy management (EMS) or supervisory control of hybrid electric vehicles (HEV) has been the subject of a large amount of scientific effort in the last years (e.g. [1], [2]). Indeed, it is widely recognized that optimizing the energy flows between the HEV components offers a large room for improving its performance in terms of tank-to-wheel energy efficiency and possibly local emissions. However the complexity of the energy interactions requires that the EMS is designed on a systematic and general base, rather than heuristically based on ad-hoc control rules. Optimal-control based techniques emerge as an effective framework to EMS, both off line (Dynamic Programming (DP) e.g. [3], [4], [5], Pontryagin's Minimum Principle (PMP) e.g. [6], [7], [8]) and on line (Equivalent Consumption Minimization Strategy (ECMS) e.g. [9], [10], [11], [12], [13], [14]).

Usually the optimality criterion is the fuel consumption (and possibly local pollutant emissions), with the main constraint on battery charge-sustaining operation. One often hidden assumption is that HEV system is under thermal equilibrium. However, thermal transients are in HEVs even more important than in conventional engine-propelled vehicles, since the engine itself is subject to stop-and-start phases and engine temperature has an influence on local emission and fuel consumption rates. Similar considerations are valid for other components (notably power electronics, batteries, and electric machines). Few publications have reported researches aimed at integrating Thermal Management Strategies (TMS) in the more general framework of EMS. In [15] the analysis is very specific to the particular application (a hybrid-solar-electric vehicle) and hybrid configuration (series hybrid). In [16] the light-off time of an electrical heated catalyst is included in the optimisation of an HEV using a natural gas engine. In spite of these early efforts, a general and systematic coverage of the topic is thus lacking.

To make the supervisory problem even more challenging, in complex HEVs not only fuel power is combined to electric power through mechanical power, but also thermal power participates to the exchanges (Fig. 1). Thermal power lost by the engine is accumulated in thermal capacities (water, oil, catalyst) and possibly used to heat the cabin. Some engine performance, notably including fuel consumption and pollutant emissions, depend on the thermal level of the thermal capacities. Moreover, thermal power might be accumulated in heat accumulators and used later to heat the engine. Exhaust thermal power otherwise lost can be partially converted using recovery systems (Rankine-cycle circuits, thermoelectric modules, etc.) to produce electric power. Moreover, some recovery systems might re-inject thermal power into the engine system. Mechanical, electrical, and thermal powers demand for the accessories of course play a substantial role in the picture.

Some steps toward the management of these power flows in the framework of an optimal EMS are reported in this paper and in the companion paper [17]. The latter focuses on the three-way catalyst thermal state and its management for limiting pollutant emissions. In this paper the focus is on integrating the engine temperature as a state variable in the EMS. A model of the influence of engine temperature on fuel consumption is presented in Section II, together with Section III. A simple but sufficiently accurate thermal model is presented. On this basis, a PMP-based EMS is derived to include engine temperature (Section III) through the introduction of a second costate besides that adjoint to the battery state of charge (SOC). With the previous model, it is possible to test the strategy directly only using Matlab, some results of offline optimization are presented in Section IV.

II. Control-oriented modelling

The temperature of the engine has a great influence on the performance of the engine in terms of consumption, as well as pollutant emissions. The current study mainly focuses on the consumption aspect. It is well know from [18] that the temperature acts on friction as well as on combustion. First a warm engine model is presented then the two extra losses due to cold temperature will be described. In this work the

978-1-4244-8218-4/10/$26.00 ©2010 IEEE

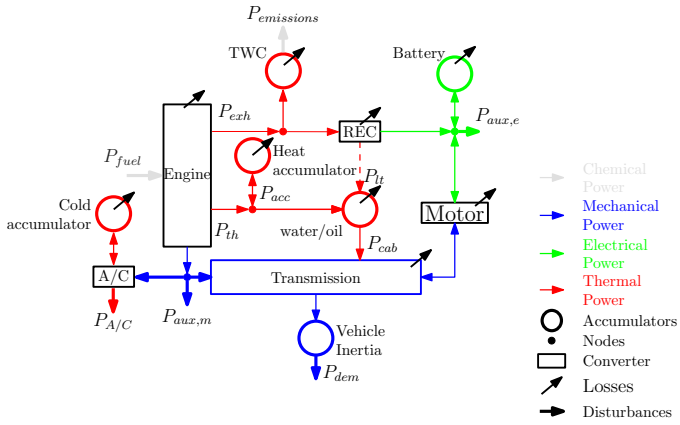

Fig. 1. Future thermal management

oil temperature is considered as representative of the overall engine thermal level. In this section the values which are given for warm conditions are symbolized by a superscript $*$.

A. Warm engine modelling

In this section the warm-engine is modelled as a quasistatic system where the engine effective torque T_e and the engine speed N_e are the input variables and the fuel consumption rate $\dot{m}_{fuel}$ is the output variable.The model integrates a fuel consumption map,

$$\dot{m}^*_{fuel} = \dot{m}^*_{fuel}(T^*_i, N_e) \tag{1}$$

where the indicated torque is given by

$$T^*_i = T_e + \frac{P^*_{fric}(N_e)}{N_e} \tag{2}$$

and the friction power P_{fric} is expressed as a function of N_e as stated in [19],

$$P^*_{fric}(N_e) = \text{tfmep}^*(N_e) \cdot V_d \cdot \frac{N_e}{n_r} \tag{3}$$

with V_d the total displaced volume, n_r the number of crank revolutions for each power stroke per cylinder and tfmep^* the total friction mean effective pressure.

B. Cold-engine friction model

Several publications have treated the modeling of thermal influence on engine friction losses (e.g. [20], [21], [22], [23], [24]). As in [22], the model used in this paper uses oil viscosity as the link between temperature and friction losses. Actually, the lower the temperature is, the higher the viscosity is. Consequently, a different expression of tfmep depending on the oil temperature θ_{oil} is used,

$$\text{tfmep}(N_e, \theta_{oil}) = \text{tfmep}^*(N_e) \cdot \left(\frac{\nu(\theta_{oil})}{\nu^*}\right)^d \tag{4}$$

where ν^* is the viscosity for a warm engine. The coefficient d allows to calibrate the model using experiments. Using (3) and (4) the final expression of P_{fric} is,

$$P_{fric}(N_e, \theta_{oil}) = P^*_{fric}(N_e) \cdot \left(\frac{\nu(\theta_{oil})}{\nu^*}\right)^d \tag{5}$$

C. Losses during the combustion

As it is well known, due to the low temperature of the cylinder during cold-start operation, unburnt hydrocarbons appear. Consequently, to obtain the desired torque more fuel than under warm conditions is needed. Therefore as a first approximation, a multiplying factor $\psi(\theta_{oil})$ is added to the consumption model. Using this factor, P_{fuel} which represents the power contained in the fuel can be written as

$$P_{fuel}(T_e, N_e, \theta_{oil}) = LHV \cdot \dot{m}^*_{fuel}(T_i, N_e) \cdot \psi(\theta_{oil}) \tag{6}$$

$$T_i = T_e + \frac{P_{fric}(N_e, \theta_{oil})}{N_e} \tag{7}$$

with LHV the lower heating value of the fuel. The function $\psi(\theta_{oil})$ tends to 1 as the temperature θ_{oil} tends to $\theta^*_{oil} = 87°\text{C}$. In the next section the model of the temperature is described.

D. Modelling the oil temperature

Modelling the oil temperature is a complex task as it has to be accurate but in the same time simple enough to be included in the EMS. That is why a first-order model was chosen. It includes two main sources of heat, P_{fric} and P_{gw}, the subscript for the latter, gw, stands for gas to wall and represents the heat dissipated through the combustion chamber. The impact of the oil/water exchanger is neglected and therefore it is not necessary to add the water temperature as a further state. This leads to the following model,

$$MC\frac{d\theta_{oil}}{dt} = a \cdot P_{fric} + b \cdot P_{gw} - c \cdot (\theta_{oil} - \theta_{ext}) \tag{8}$$

this model is reformulated as follows for identification purpose,

$$\frac{d\theta_{oil}}{dt} = \alpha \cdot P_{fric} + \beta \cdot P_{gw} - \delta \cdot (\theta_{oil} - \theta_{ext}) \tag{9}$$

Here α, β, δ and MC, which is the thermal capacitance, represent the coefficients of the model determined using experiments, θ_{ext} is the room temperature and is considered as a constant value. The expression of P_{fric} is given by (5), while P_{gw} is derived from a power balance across the engine,

$$P_{gw} = P_{fuel} - P_e - P_{fri} - P_{exh} \tag{10}$$

with

$$P_{exh} = (1 + \text{AFR}) \cdot \dot{m}_{fuel} \cdot C_{pexh} \cdot \theta_{exh} \tag{11}$$

AFR being the air-fuel ratio and P_{exh} the power of the exhaust gas. The exhaust temperature θ_{exh} is mapped as a function of N_e, T_e. The mechanical effective power is given by

$$P_e = T_e \cdot N_e \tag{12}$$

with P_e the effective power.

TABLE I
MODEL PARAMETERS

Parameter	Value
d	0.3
α	$6.1396.10^{-5}$
β	$3.7395.10^{-6}$
δ	0.0014

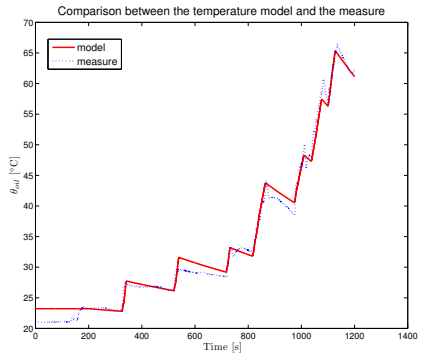

Fig. 2. Comparison between oil temperature model and experiment

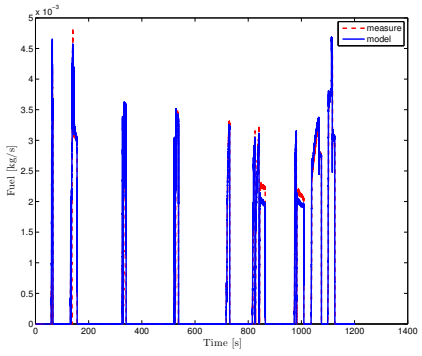

Fig. 3. Comparison between fuel consumption model and measure

E. Model Validation

The experimental tool used is an HEV where everything but the engine is emulated by real-time running models (see Section IV). Using this test bed a NEDC cycle in cold condition was performed. As it can be seen in Fig. 2-3, the model is a good approximation of the experiment with the model parameters listed in Table I. The difference visible at the start of the experiment for the oil temperature comparison is due to the establishment of the heat transfer between the combustion chamber and the engine.

III. SUPERVISORY CONTROL

After modelling the effects of the temperature, the paper is focused on supervisory control. An optimal-based control is extended to take into account the engine temperature.

A. Optimal control problem

The energy-management strategy considered is based on PMP (applicable off line) or on its online counterpart ECMS. In the usual formulation, not depending on engine temperature, the EMS output (e.g., the engine torque T_e in the case of a parallel hybrid) is calculated by minimizing an Hamiltonian function,

$$T_e(t) = \arg\min_{T_e} H^*(T_e, N_e, t) \tag{13}$$

with

$$H^*(T_e, N_e, t) = P_{fuel}(T_e, N_e) + s \cdot P_{elec}(T_e, N_e, t) \tag{14}$$

in its simplest formulation (i.e., not considering additional drivability or state constraints). In (14), P_{elec} is the battery inner electrochemical power (proportional to SOC variation) and the Lagrange multiplier s is known as the equivalence factor. This form is relatively simple as there is only one state variable and the variation of s is neglected. In this case, the fuel rate depends only on engine torque and engine speed. The contribution of this paper consists in adjoining the variation of the additional state variable, the engine temperature. Similarly to SOC variation, this term is adjoint through a second costate, $p(t)$,

$$\begin{aligned} H(T_e, N_e, \theta_{oil}, t) =& P_{fuel}(T_e, N_e, \theta_{oil}) + s \cdot P_{elec}(T_e, N_e, t) \\ &+ p(t) \cdot P_{th}(T_e, N_e, \theta_{oil}) \end{aligned} \tag{15}$$

with the dynamics of p being known (see below). In (15) P_{th} is a reformulation of engine temperature variation in power units,

$$P_{th} = -MC \cdot \dot{\theta}_{oil} \tag{16}$$

This new state was chosen in order to work exactly as P_{elec}.When P_{elec} is negative the battery is charging and when P_{elec} is positive the battery is discharging. Looking at (16), the same behaviour is reproduced i.e. P_{th} is negative if $\dot{\theta}_{oil}$ is positive, which corresponds to charging the thermal capacity.

The Euler-Lagrange equation associated to the new costate $p(t)$ is,

$$\dot{p}(t) = -\frac{\partial H(T_e, N_e, \theta_{oil}, t)}{\partial\left(-MC \cdot \theta_{oil}\right)} \tag{17}$$

$$= \frac{1}{MC} \cdot \frac{\partial H(T_e, N_e, \theta_{oil}, t)}{\partial \theta_{oil}} \tag{18}$$

The explicit derivation of $\dot{p}(t)$ is cumbersome but straightforward, thus the details are not provided in this paper.

B. Offline optimization

To assess the potential gains due to considering the thermal transients explicitly in the Hamiltonian, an offline optimization of the supervisory control rule (13) is performed. The optimal solution is characterized by two optimal values for s and the initial condition of $p(t)$, namely p_0. The former is determined by the value of the SOC at the final time t_f, which has to be equal to the initial value (charge-sustaining operation). However, for p_0 there is no such simple criterion. Ideally, p_0 should be such that $p(t_f) = 0$. However, due to rounding errors in the practical implementation of differential equations

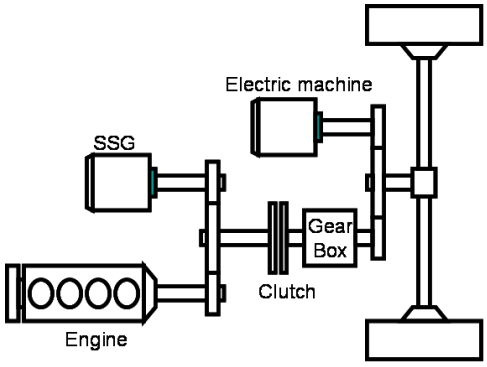

Fig. 4. The parallel hybrid architecture analyzed in this study.

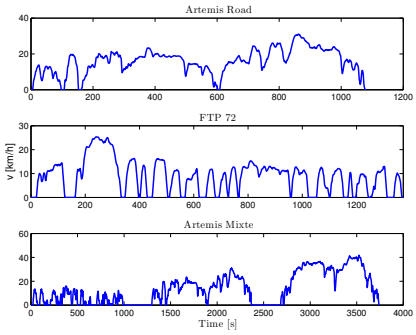

Fig. 5. Drive cycles used for the comparison

such (17), such condition proves not to be effective. Therefore, the method used here consists of testing a large range of p_0 values and for each of them finding the value of s that guarantees the right final SOC using a zero-finding algorithm. Then, the "optimal" p_0 is chosen as the one that minimizes the overall fuel consumption.

IV. Discussion

In this section three aspects of this new control strategy are investigated in simulation, firstly a comparison of consumption for several drive cycles, secondly a more detailed study on the Artemis Road cycle, and finally a sensitivity analysis of the results with respect to the value of p_0. The results are obtained for a parallel hybrid (Fig. 4) with a $2l$ gasoline turbocharged engine, this architecture whose presented in [13].

A. General results

Using the model given in Section II several tests are conducted using three different drive cycles, such as Artemis Road, FTP 72 and Artemis Mixte (Fig. 5). In each case the HEV is in charge-sustaining mode (CS) with $SOC(0) = 50\%$. The fuel consumption with "warm engine" (i.e., initial temperature close to thermal equilibrium) is compared with the fuel consumption for the "cold-engine" case ($\theta_{oil}(0) = 25°C$) using the ECMS as in Section III-A, with and without considering the thermal power contribution. As summarized in Table II, the gain in fuel consumption obtained with (15) instead of (14) can be has high as 2.8%, but it drops virtually to zero for the Artemis Mixte cycle. However, another performance could be investigated, which is the energy released by the exhaust gases. The amount of energy transmitted through the exhaust gases is used to activate the after-treatment system of the engine. For a cold-start purely ICE (no HEV) operation it was experimentally observed that when the catalyst temperature is $\approx$ 300°C the oil temperature is at $40 - 50$°C. Thus a light-off time has been defined as the time required to get $\theta_{oil} = 45$°C. Clearly it is a "raw" comparison but it is sufficient to look at the general trend. A more detailed study on this topic is done in the companion paper. Table IV shows that in each case the "light-off" time is reduced using (15). Moreover for the Artemis Mixte cycle, even if there is not a very high improvement on fuel consumption, there is a good improvement from the "light-off" time point of view.

TABLE II
Comparison on consumptions

	Units	Artemis Road	FTP 72	Artemis Mixte
Warm engine	(l/100 km)	4.36	3.38	6.31
Cold engine w/o $p(t)$	(l/100 km)	4.81	3.87	6.60
Cold engine with $p(t)$	(l/100 km)	4.67	3.79	6.55
gain	(%)	2.81	2.14	0.64

TABLE III
"Light-off" time

		Artemis Road	FTP 72	Artemis Mixte
light-off time (s)	without $p(t)$	774	463	1372
	with $p(t)$	379	260	407

B. The Artemis Road cycle

In this section a more detailed comparison is presented for the Artemis Road cycle. The three system variables T_e, SOC, and θ_{oil}, are shown in Fig. 6-8. In each case a comparison between the use of (15) and (14) is made. Using the proposed strategy the oil temperature tends to be higher and starts increasing at the beginning of the cycle. On the contrary using (14) the temperature is relatively low and starts increasing later. This behaviour is well-explained looking at the SOC. For the baseline ECMS, the SOC decreases until a relatively low level and starts increasing until it reaches the final target value. The time corresponding to the recharge of the battery is the same time when the oil temperature increases. For the temperature-sensitive ECMS, the SOC is kept closer to the final target value all along the cycle. To achieve that, the engine has to be started more often, which is the case as shown by the engine torque plot (Fig. 6). A further comparison concerns the energy transmitted through the exhaust gases . More precisely, Fig. 9 shows the ratio of the thermal power of the exhaust gases over the total power contained in the fuel, during the "light-off" time defined in Section IV-A. Obviously a larger part of the total power is sent through the exhaust gases using the temperature-sensitive ECMS. Moreover, in Table IV the ratio of the total energy transmitted to the exhaust gases is

TABLE IV
RATIO OF THE TOTAL ENERGY TRANSMITTED TO THE EXHAUST GASES

		Artemis Road	FTP 72	Artemis Mixte
E_{exh}/E_{fuel} (%)	without $p(t)$	15.6	19.4	9.1
	with $p(t)$	18.5	22.5	19.7

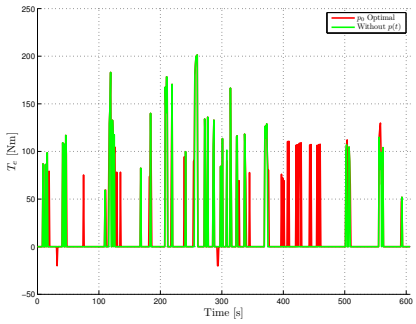

Fig. 6. Engine torque for the baseline ECMS and the temperature-sensitive ECMS

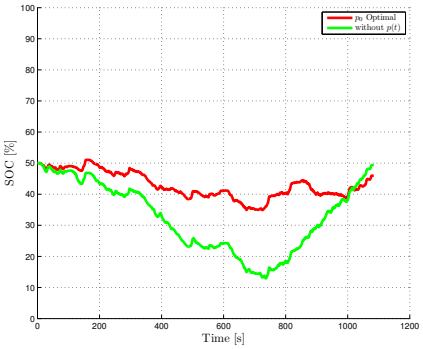

Fig. 7. State of charge for the baseline ECMS and the temperature-sensitive ECMS

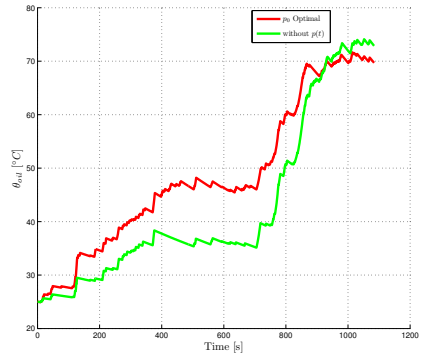

Fig. 8. Oil Temperature for the baseline ECMS and the temperature-sensitive ECMS

represented and using (15) the ratio are larger than using (14). Using this strategy proves to be an effective mean of acting on the energy balance of the engine.

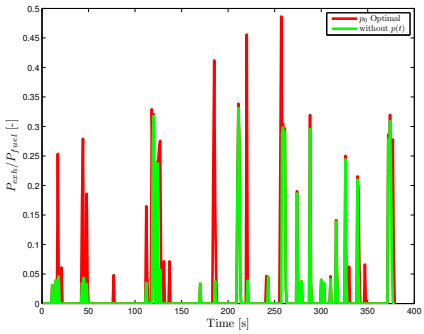

Fig. 9. $P_{exhaust}$ over P_{fuel} for the baseline ECMS and the temperature-sensitive ECMS

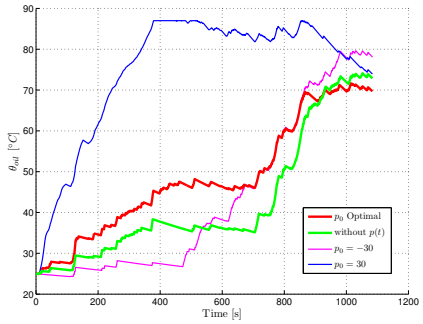

Fig. 10. Oil Temperature for different values of p_0

C. Sensitivity analysis to p_0

In this section the effects of the value p_0 are described based on Fig. 10-12. In these figures $\theta_{oil}(t)$, SOC(t) and $p(t)$ are represented for different values of p_0, namely the optimal value ($p_0 = 5$), $p_0 = -30$, $p_0 = 30$, and when $p(t)$ is not used (i.e. the baseline ECMS). Only the upper and lower bounds of p_0 used are represented. The resulting trajectories can be regarded as enveloping the trajectories obtained with any other intermediate value of p_0. Looking at Fig. 10-12 two domains can be extracted from the results, the first one when $p0 > 0$ and the second one when $p0 < 0$. A positive value of $p0$ yields a higher oil temperatures and a higher SOC values during the cycle. Contrarily, a negative value of $p0$ tends to reduce the oil temperature and the average value of the SOC. This was expected as stated in Section III-A and the simulation confirms that the multiplier $p(t)$ behaves similarly to the multiplier s. The time evolution $p(t)$ shows that $p(t_f)$ tends to zero although the zero value is not exactly reached for the "optimal" choice of p_0, as explained in Section III-B.

V. CONCLUSIONS

In this paper a combined thermal management and energy management strategy for hybrid electric vehicles is derived from the well-known ECMS by adding a new state variable representing the engine temperature. The use of the proposed strategy proves to be effective in reducing the fuel consumption over several cold-start driving cycles. Moreover, thermal

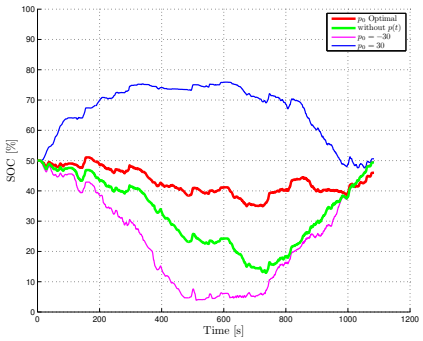

Fig. 11. State of charge for different values of p_0

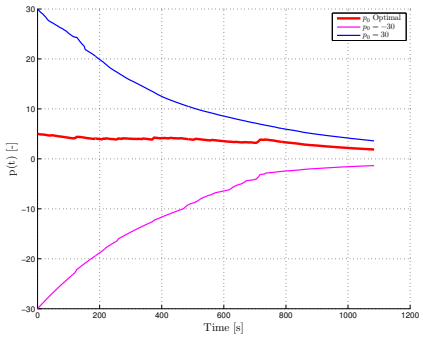

Fig. 12. $p(t)$ for different values of p_0

transient of the system is enhanced since the catalyst light-off time is sensibly reduced. The latter result is due to a more effective energy balance of the engine and it potentially leads to a substantial reduction of the pollutant emissions. The ideas introduced in this paper can be extended to include other thermal states of modern hybrid electric vehicles, leading to a completely integrated thermal management and energy management strategy. The latter should be able to cope not only with driver's traction demands but also with vehicle-level demands such as cabin heater or air conditioning. Further work is also needed in order to transform the strategy presented in a fully online strategy, i.e., with a continuous adaptation of the new adjoint state (multiplier) introduced.

REFERENCES

[1] A. Sciarretta and L. Guzzella, "Control of hybrid electric vehicles," *IEEE Control Systems Magazine*, vol. 27, no. 2, pp. 60–70, 2007.

[2] P. Pisu and G. Rizzoni, "A comparative study of supervisory control strategies for hybrid electric vehicles," *IEEE Transactions on Control Systems Technology*, vol. 15, no. 3, pp. 506–518, 2007.

[3] J. Peng, "Modeling and Control of a Power-Split Hybrid Vehicle," *IEEE Transactions on Control Systems Technology*, vol. 16, no. 6, 2008.

[4] G. Ao, J. Qiang, H. Zhong, X. Mao, L. Yang, and B. Zhuo, "Fuel economy and NOx emission potential investigation and trade-off of a hybrid electric vehicle based on dynamic programming," *Proceedings of the Institution of Mechanical Engineers, Part D: Journal of Automobile Engineering*, vol. 222, no. 10, pp. 1851–1864, 2008.

[5] L. Johannesson, M. Asbogard, and B. Egardt, "Assessing the potential of predictive control for hybrid vehicle powertrains using stochastic dynamic programming," *IEEE Transactions on Intelligent Transportation Systems*, vol. 8, no. 1, p. 71, 2007.

[6] G. Rousseau, D. Sinoquet, and P. Rouchon, "Constrained optimization of energy management for a mild-hybrid vehicle," *Oil & Gas Science and Technology-Revue de l'IFP*, vol. 62, no. 4, pp. 623–634, 2007.

[7] G. Paganelli, T. Guerra, S. Delprat, J. Santin, M. Delhom, and E. Combes, "Simulation and assessment of power control strategies for a parallel hybrid car," *Proceedings of the Institution of Mechanical Engineers, Part D: Journal of Automobile Engineering*, vol. 214, no. 7, pp. 705–717, 2000.

[8] A. Sciarretta, M. Back, and L. Guzzella, "Optimal control of parallel hybrid electric vehicles," *IEEE Transactions on control systems technology*, vol. 12, no. 3, pp. 352–363, 2004.

[9] D. Ambühl, A. Sciarretta, C. Onder, L. Guzzella, S. Sterzing, K. Mann, D. Kraft, and M. Küsell, "A causal operation strategy for hybrid electric vehicles based on optimal control theory," in *Proc of the 4th Symposium Hybrid Vehicles and Energy Management, Braunschweig*, 2007.

[10] Q. Gong, Y. Li, and Z. Peng, "Trip-Based Optimal Power Management of Plug-in Hybrid Electric Vehicles," *IEEE Transactions on Vehicular Technology*, vol. 57, no. 6, pp. 3393–3401, 2008.

[11] J. Kessels, M. Koot, P. van den Bosch, and D. Kok, "Online Energy Management for Hybrid Electric Vehicles," *IEEE Transactions on Vehicular Technology*, vol. 57, no. 6, pp. 3428–3440, 2008.

[12] A. Kleimaier and D. Schroder, "An approach for the online optimized control of a hybrid powertrain," in *IEEE Advanced Motion Control Conference*, 2002.

[13] A. Chasse, G. Hafidi, P. Pognant-Gros, and A. Sciarretta, "Supervisory control of hybrid powertrains: an experimental benchmark of offline optimization ond online energy management," in *in Proc of the IFAC Workshop on Engine and Powertrain Control, Simulation and Modelling, Rueil-Malmaison, France, Nov.30-Dec.2, 2009*, 2009.

[14] A. Chasse, A. Sciarretta, and J. Chauvin, "Online optimal control of a parallel hybrid with costate adaptation rule," *accepted for publication in 6th IFAC Symposium Advances in Automotive Control*, 2010.

[15] I. Arsie, G. Rizzo, and M. Sorrentino, "Effects of engine thermal transients on the energy management of series hybrid solar vehicles," *Control Engineering Practice*, 2010.

[16] J. Kessels, D. Foster, and W. Bleuanus, "Towards Integrated Powertrain Control: Thermal Management of NG Heated Catalyst System," in *Proc of the International Conference on Advances in Hybrid Powertrains, Rueil-Malmaison, France, Nov. 25-26,2008.*

[17] A. Chasse, G. Corde, and A. Del Mastro, "Online optimal control of a parallel hybrid with after-treatment constraint integration." VPPC2010, 2010.

[18] R. Van Basshuysen and F. Schäfer, *Internal combustion engine handbook: basics, components, systems, and perspectives*. SAE International, Warrendale, PA, 2004.

[19] J. Heywood, *Internal Combustion Engine Fundamentals*. McGraw-Hill, Inc, 1988.

[20] K. Patton, R. Nitschke, and J. Haywood, "Development and evaluation of a friction model for spark ignition engines," *SAE, 890836*, 1989.

[21] P. Shayler, S. Christian, and T. Ma, "A model for the investigation of temperature, heat flow and friction characteristics during engine warm-up," *SAE International, 931153*, 1993.

[22] S. Bohac, D. Baker, and D. Assanis, "A global model for steady state and transient SI engine heat transfer studies," *SAE transactions*, vol. 105, pp. 196–214, 1996.

[23] L. Jarrier and D. Gentile, "Simulation du comportement thermique transitoire d'un moteur combustion interne et allumage commandé," *Revue Gnrale de Thermique*, vol. 36, no. 7, pp. 520 – 533, 1997.

[24] D. Sandoval and J. Heywood, "An Improved Friction Model for Spark-Ignition Engines," *SAE, 2003-01-0725*, 2003.